



Technical Sciences  
Academy of Romania  
[www.jesi.astr.ro](http://www.jesi.astr.ro)

## Journal of Engineering Sciences and Innovation

Volume 2, Issue 4/ 2017, pp. 70-76  
<http://doi.org/10.56958/jesi.2017.2.4.70>

D. Chemical Engineering, Materials Science and  
Engineering, Natural Resources

Received 21 September 2017

Accepted 6 December 2017

Received in revised form 20 November 2017

### Research on elaboration of metallic foams based on Ni alloy powders

VIDA-SIMITI IOAN<sup>\*1</sup>, THALMAIER GYORGY, SECHEL NICULINA

<sup>1</sup>Technical University of Cluj-Napoca, Muncii Bvd., no.103-105, Cluj-Napoca, 400641,  
Romania

**Abstract.** For this study, 125 to 630  $\mu\text{m}$  solid spherical particles of NiCrSiB powders were used. To shape the macro porous structure, space holders were used (spherical particles of polystyrene). Metal foam structure arise after sintering the powder in vacuum ( $1.3 \cdot 10^{-3}$  Pa) at a temperature of 1000 °C, for 30 minutes. Thus, porous metal foam is obtained of which the structure is composed of the interparticle open pores and the pores formed by the space holders. The structure of metal foams has been investigated by optical and electronic microscopy. Densities from 3.71 to 1.78 [ $\text{g}/\text{cm}^3$ ] were obtained. There is a linear dependence of thermal conductivity as function of temperature. The heat transmission is mainly by conduction at the interparticle necks. The sound attenuation is a function of frequency. Maximum sound absorption coefficient for samples obtained is 0.38 at the frequency of 1000 Hz.

**Keywords:** Metallic foams, solid particles, space holders.

#### 1. Introduction

Metal foams are a group of sintered cells with solid edges and faces thus defining a cellular structure [1] which combines the basic material properties with those of the cellular materials [2]. Open-pore foams have a irregular structure with high specific surface. This led to their use in many applications such as catalytic supports, heat exchangers, high temperature resistant filters, battery electrodes and electromagnetic absorbers. Such a feature of foams in general and aluminum foams in particular, consists of a combination of properties not seen in other materials: high compressive strength, low density and ability to support a permanent plastic deformation in a constant effort. Two main types have been suggested for use: as impact absorbers and as light structural materials [2]. The main quality of cellular

\*Correspondence address: [Vida.Simiti@stm.utcluj.ro](mailto:Vida.Simiti@stm.utcluj.ro)

metallic materials is their versatility. As interesting combinations of physical and mechanical properties - good energy absorbers, low specific weight, good thermal or sound insulators - they reach high functional performance necessary in the automotive industry, aerospace [3, 4], naval, civil and industrial construction [1, 5, 6]. Current researches open new horizons and approached a wide variety of topics such as: amorphous metal foams materials (e.g. iron alloys) [7, 8], composite metal foams with hollow steel spheres [9], tin-lead metal foams [10], and the development of their physical and mechanical properties [11-14]. Attempts have been made in structural modeling [15-17] of metal foams to predict their properties.

The paper aims to study the links between technological factors and properties of the foams obtained by the space holder method

## 2. Materials and methods used

For this study we used spherical NiCrSiB superalloy powder particles. The nickel based alloy powder, the material used in experimental tests to obtain metallic foams, with 125-630  $\mu\text{m}$  particle size was obtained by argon gas atomization. The chemical composition of the powder is shown in Table 1.

Table 1. The chemical composition of NiCrSiB powder

Element	Ni	Fe	Cr	Si	B
[%]wt.	70,19	12,34	7,08	6,73	3,66

The sorted powder was freely poured into ceramic molds with inner diameter of 17 mm and height of 28 mm. The molds were placed on a ceramic support and introduced into the sintering furnace.

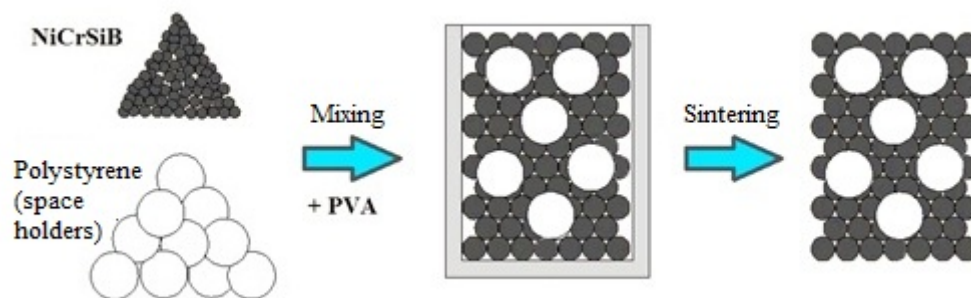


Fig.1 Schematic illustration of fabrication route of the NiCrSiB foam using the space holder method.

In the case of powder sintering using space holders, the polystyrene is mixed with an organic binder and the metallic powder. The role of the organic binder is to maintain the metal structure after removing the space holders.

For the large pores, polystyrene particles with the size of 2 to 2.5 mm were used. The melting temperature of polystyrene is 240 °C, density of 1.01 to 1.04 g/cm<sup>3</sup> and its thermal decomposition occurs at a temperature of 390 °C.

NiCrSiB and polystyrene particles were mixed, homogenized for 10 minutes and bonded with a binder before sintering: polyvinyl alcohol, a synthetic hydrophilic polymer, soluble in water, with melting point at 180-190 °C and decomposition temperature at 200 °C. the resulted mix was poured into cylindrical molds of alumina and sintered in vacuum ( $1.3 \cdot 10^{-3}$  Pa) at a temperature of 1000 °C for 30 minutes, the optimal parameters determined by a prior sintering study [18].

To eliminate the polyvinyl alcohol and polystyrene, two holding steps of 10 minutes were required at 200 °C and 400 °C, the used sintering cycle is shown in Figure 2.

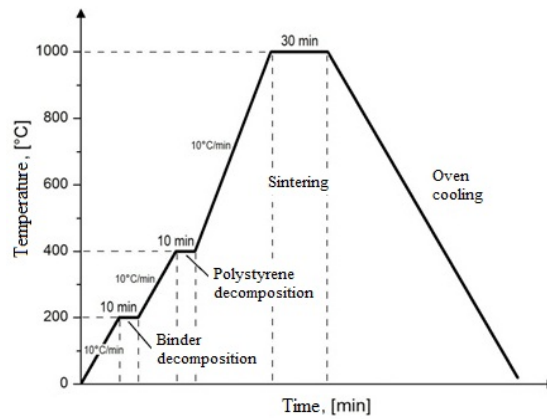


Fig.2 Sintering diagram of the NiCrSiB foam.

### 3. Experimental results

In the images presented in Figure 3, the structures of the obtained samples can be seen. In Figure 3.a, one can see an overview of the sample with macro pores of 2 – 2.5 mm into the body of the sintered structure.

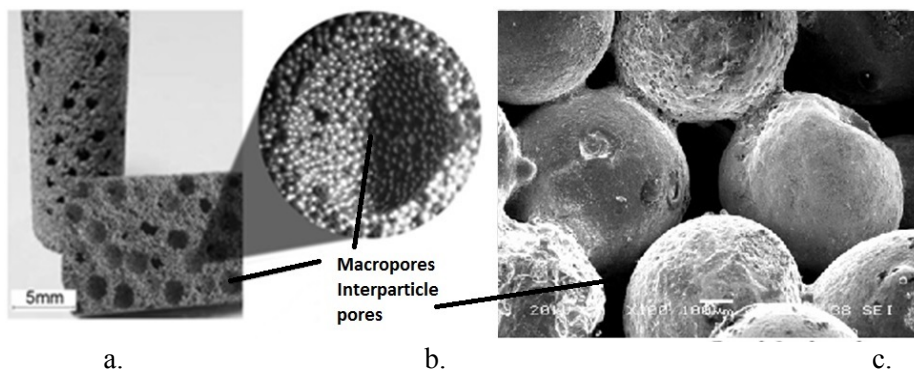


Fig. 3. Images of the bi-porous metal foam structures.

Figure 3.a represents a detailed optical image, in section, where the sintered structure of the particles and a macro pore formed by removing the space holder can be seen. In Figure 3.b, also an optical image, a top view of a macro pore obtained by removing the pore forming agent is presented. One can see the micro pores between the sintered particles and the internal pores from the hollow particles. In Figure 3.c, a SEM image is presented, representing sintered particles from the bi-porous structure of the metal foam and the sintering necks formed between them. In the top right part of a macro pore is viewable.

Density and porosity of the obtained samples are given in Table 4.9 for samples obtained with solid spherical particles.

Porosity  $P$  (porous phase) consists of:  $P = P1 + P2$ , where:  $P1$  - porosity given by micropores (between the sintered powder particles);  $P2$  - porosity given by macropores (macropores formed by polystyrene particles);

The macropores have relatively the same size in all samples and micro pores depend on the particle size.

Table 2. Porosity and density of the samples

Particle size range, $[\mu\text{m}]$	Porosity, $P$ [%]	Sintered density, $\rho_{sp}$ [ $\text{g}/\text{cm}^3$ ]	Relative density, $\rho_{sp}/\rho_m$
125-200	52	3,71	0,48
200-315	59	3,13	0,41
315-400	65	2,72	0,35
400-500	73	2,11	0,27
500-630	77	1,78	0,23

From Table 2 it can be seen the difference in porosity and density of the samples obtained from powders using space holders. Thermal conductivity dependence on temperature and relative density for the samples from powders with solid particles obtained using space holders is shown in Figure 4.

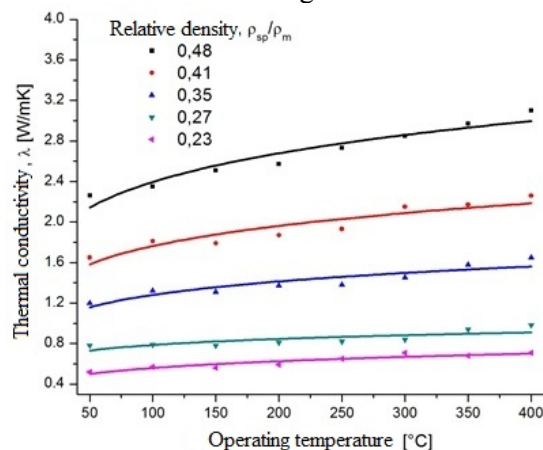


Fig. 4. Influence of testing temperature on thermal conductivity at different relative densities.

The mode of heat transmission through porous structures is mainly by thermal conduction through interparticle necks. By using space holders and lower the relative density of samples a decrease in thermal conductivity occurs. With increasing operating temperature, thermal conductivity increases, but this increase is less evident with decreasing relative density (Figure 4).

Porous phase growth by increasing the powder particle size makes the thermal conductivity decrease. As expected, the thermal conductivity is much lower in the porous phase than the solid phase. Thus, the thermal conductivity decreases with decreasing relative density and increasing porosity.

Loss of sound energy, respectively sound absorption in porous materials is caused mainly by the air friction and its oscillation in the pores of the material. For effective sound absorption the material should have a porous structure, the pores must be open to the exterior and communicate with each other. Sound absorption in porous sample (attenuation) is given by equation 1.

$$\alpha = \frac{I_a}{I_i} \quad (1)$$

where:  $\alpha$  is sound absorption coefficient,  $I_a$  – the intensity of the absorbed acoustic waves, and  $I_i$  – the intensity of the incident acoustic waves.

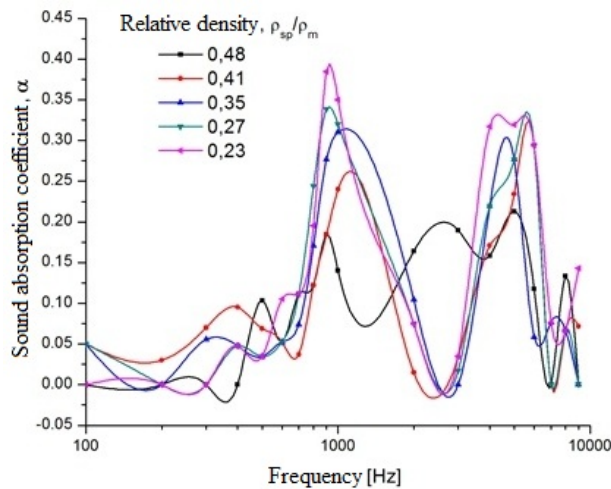


Fig. 5 Sound absorption coefficient variation of samples function of noise frequency at different relative densities.

By lowering the relative density through the use of space holders is found an improvement in sound absorption for the frequency of 1000 Hz, and a decrease in absorption at frequencies of 2000 and 3000 Hz (Figure 5 a) compared with samples obtained without space holders. Maximum sound absorption coefficient for the samples obtained from powders with solid particles and space holders is 0.38, at

the frequency of 1000 Hz. Decreasing relative density increases the absorption of sound at certain frequencies. Sound attenuation is function of frequency and relative density, respectively the grain size fraction of the powder used. With decreasing relative density sound absorption coefficient increases.

#### 4. Conclusions

Good quality nickel superalloy foams were obtained using the space holder method. The polystyrene particles were successfully removed at 400 °C during the sintering cycle. The porosity slightly increase

Thermal conductivity decreases with decreasing the relative density. Heat transfer being reduced with increasing temperature a difference in conductivity occurs between the temperature of 50 °C and 400 °C. This difference is smaller as the porosity increases. The thermal conductivity lies in the 0.6-3 W/mK range.

With decreasing relative density sound absorption coefficient increases. Maximum sound absorption coefficient for the samples is 0.38, at the frequency of 1000 Hz.

#### References

- [1]. J. Banhart, *Manufacture, characterization and application of cellular metals and metallic foams*. Progress in Material Science, **46**, 2001, p. 559-632.
- [2]. M.F. Ashby, A.G. Evans, N.A. Fleck, L.J. Gibson, J.W. Hutchinson and H.N.G. Wadley, *Metal Foams: A Design Guide*, Boston, Butterworth-Heinemann, 2000.
- [3]. A.G. Evans, J.W. Hutchinson and M.F. Ashby, *Multifunctionality of Cellular Metal Systems*, Progress Mater. Sci., **43**, 1999, p. 171-221.
- [4]. C. Korner and R.F. Singer, *Processing of Metal Foams - Challenges and Opportunities*. Metal Matrix Composites and Metallic Foams – EUROMAT, Wiley-VCH., 1999.
- [5]. F. Baumgartner, I. Duarte, J. Banhart, *Industrialization of P/M foaming process*, Advanced Engineering Materials, **2**, 2000, p. 168-174.
- [6]. J. Banhart, *Aluminium foams for lighter vehicles*, International Journal of Vehicle Design, **37**, 2005, p. 114-125.
- [7]. A. H. Brothers, D.C. Dunand, *Amorphous metal foams*, Scripta Materialia, **54**, 2006 p. 513-520.
- [8]. M. D. Demetriou, G. Duan, C. Veazey, K. De Blauwe, W. L. Johnson, *Amorphous Fe-based metal foam*, Scripta Materialia, **57**, 2007, p. 9-12.
- [9]. B. P. Neville, A. Rabiei, *Composite metal foams processed through powder metallurgy*. Materials and Design, **29**, 2008, p. 388-396.
- [10]. A. E. Belhadja, S. A. Kaouaa, M. Azzaza, J. D. Bartoutb, Y. Bienvenu, *Elaboration and characterization of metallic foams based on tin-lead*, Materials Science and Engineering A, **494**, 2008, p. 425-428.
- [11]. S. Lee, F. Barthelat, N. Moldovan, H. D. Espinosa, H.N.G. Wadley, *Deformation rate effects on failure modes of open-cell Al foams and textile cellular materials*, International Journal of Solid and Structures, **43**, 2006, p. 53-73.
- [12]. X.Y. Zhoua, J. Li, B. Longa, D.W. Huo, *The oxidation resistance performance of stainless steel foam with 3D open-cell network structure at high temperature*. Materials Science and Engineering A, **435-436**: 40-45, 2006.
- [13]. D. Ruan, G. Lu, L.S. Ong, B. Wang, *Triaxial compression of aluminium foams*, Composites Science and Tehnology, **67**, 2007, p. 1218-1234.
- [14]. L. Peroni, M. Avalle, M. Peroni, *The mechanical behavior of aluminium foam structures in different loading conditions*, International Journal of Impact Engineering, **35**, 2008, p. 644-658.

- [15]. M. De Giorgi, A. Carofalo, V. Dattoma, R. Nobile, F. Palano, *Aluminium foams structural modeling*, Computers and Structures, **88**, 2010, p. 25-35.
- [16]. G. Laschet, J. Sauerhering, O. Reutter, T. Fend, J. Scheele, *Effective permeability and thermal conductivity of open-cell metallic foams via homogenization on a microstructure model*. Computational Material Science, **45**, 2009, p. 597-603.
- [17]. B. Zhang, T. Kim, Y.J. Lu, *Analytical solution for solidification of closed-celled metal foams*, International Journal of Heat and Mass Transfer, **52**, 2009, p. 133-141.
- [18]. Sd I. Vida-Simiti, N. Jumate, E. Bruj, N. Sechel, Gy. Thalmaier, D. Nemeş, M. Nicoară, *Metallic Foams Obtained from Nickel Based Superalloy Hollow Spheres*, Materials Science Forum-Researches in PM, Vol. 672, 2011, p. 141-144.